BNL-35168

CONF-8405231--1

AXIAL ASYMMETRY, FINITE PARTICLE NUMBER AND THE IBA

R. F. Casten

Brookhaven National Laboratory

Upton, New York, 11973

USA

BNL--35168

DE84 016997

Invited Talk presented at the

International Workshop on Interacting Boson-Boson

and Boson-Fermion Systems

Gull Lake, Michigan

May 28-30, 1984.

AXIAL ASYMMETRY, FINITE PARTICLE NUMBER AND THE IBA

R. F. Casten
Brookhaven National Laboratory
Upton, New York 11973
USA

ABSTRACT

Although the IBA-1 contains no solutions corresponding to a rigid triaxial shape, it does contain an effective asymmetry. This arises from zero point motion in a γ-soft potential leading to a non-zero mean or rms γ. Three aspects of this feature will be discussed: 1) The relation between IBA-1 calculations and the corresponding γ. This point is developed in the context of the Consistent Q Formalism (CQF) of the IBA. 2) The dependence of this asymmetry on boson number, N, and the exploitation of this dependence to set limits on both the relative and absolute values of N for deformed nuclei. 3) The relation between this asymmetry and the triaxiality arising from the introduction of cubic terms into the IBA Hamiltonian. Various observables will be inspected in order both to determine their sensitivity to these two structural features and to explore empirical ways of distinguishing which origin of asymmetry applies in any given nucleus.

1. INTRODUCTION

It is well known[1,2] that the IBA-1 contains no triaxial solutions, that is, the corresponding classical potential never has an axially asymmetric minimum. Nevertheless, the O(6) limit corresponds to a γ-unstable potential with a mean γ near 30°. Moreover, calculated E2 branching ratios for deformed nuclei deviate from the Alaga rules. These facts suggest that, somehow, the IBA-1 must contain at least an effective asymmetry. It is the purpose here to show that this is, in fact, the case and to derive an effective γ that corresponds to a given IBA-1 calculation. The origin of this asymmetry in terms of dynamical fluctuations in a γ-soft potential will be discussed. Then, in the context of the Consistent Q Formalism[3] (CQF) of the IBA, this asymmetry will be exploited to investigate the role of finite boson number in the IBA. Finally, the relation between this asymmetry and the stable asymmetric shapes that correspond to the introduction of higher order terms in the IBA-1 Hamiltonian will be discussed.

The discussion here is a report of collaborative work. Sections 2 and 3 were done in collaboration with A. Aprahamian and D. D. Warner,[4,5] and Section 4 with K. Heyde, P. Van Isacker, and J. Jolie[6].

2. AXIAL ASYMMETRY IN IBA-1

The question of axial asymmetry in the IBA-1 can be addressed by seeking to define an effective γ value for an IBA calculation. To do this, one simply compares calculations of the same observables in the IBA and in some convenient geometric model which incorporates asymmetry. It is most convenient to carry out the IBA calculations in the CQF because, then, most results depend only on the one parameter, χ, and one simply tries to associate, to each χ value, a value for γ that gives the same result for a given observable. In the CQF, the IBA Hamiltonian for nuclei between the O(6) and SU(3) limits (only such nuclei are considered in this and the following section) is[3]

$$H = -\kappa\, Q\cdot Q - \kappa'\, L\cdot L \tag{1}$$

where

$$Q = (s^{+}\tilde{d}+d^{+}s) + (\chi/\sqrt{5})\,(d^{+}\tilde{d})^{(2)} \tag{2}$$

Since L is diagonal in the IBA basis, only the first term in H is important and thus κ is essentially an energy scale factor. The resultant wave functions and most observables therefore depend only on χ, which takes on the values $-\sqrt{35}/2 = -2.958$ in SU(3) and 0 in O(6). The transition between these limits is simply expressed in terms of a smooth variation in χ. The results of such calculations are shown in Fig. 1 for several observables and compared there with those calculated in the asymmetric rotor model[7]. A $\gamma-\chi$ correspondence can be extracted for a given observable if the calculated values pass through the same ranges. It is remarkable that this is precisely the case, even to the extent that the ratio $B(E2:2^{+}_{2}\rightarrow 0^{+}_{1})/B(E2:2^{+}_{1}\rightarrow 0^{+}_{1})$ maximizes at ≈ 0.07 in both calculations. The fact that the detailed behavior of each curve is different in the two calculations only means that the $\gamma-\chi$ correlation is non-linear. For each corresponding pair of curves in Fig. 1, a $\gamma-\chi$ correspondence can be extracted. The results are shown in Fig. 2 where it is apparent that the resultant $\gamma-\chi$ relations are nearly identical for different observables. Surely, this suggests the validity of assigning a reasonably well defined γ value to any IBA calculation with eq. (1) in the CQF.

Not surprisingly, $\gamma\rightarrow 30°$ for $\chi=0$ and drops steadily as χ increases. The fact that it does not $\rightarrow 0°$ for the SU(3) limit ($\chi = -2.958$) is a direct reflection of finite boson number effects. This is easiest to see for the energy ratio shown in Fig. 1. For axial symmetry (γ=0°) this ratio $\to\infty$ in the geometrical model but it is given by

$$E_{2_2^+}/E_{2_1^+} = [\kappa(2N-1)/(0.75\ \kappa-\kappa')] + 1 \qquad (3)$$

in the SU(3) imit of the IBA. Clearly, this can only $\to\infty$, yielding γ=0°, when $N\to\infty$. (Note: Physical values of κ and κ' have opposite sign, so the denominator in eq. (3) does not vanish.) Thus, the SU(3) limit is not a pure axial rotor, as often stated. Indeed, this is also clear from the fact that calculated branching ratios deviate from the Alaga rules, even in this limit. It is also interesting to note from the curves for N=12 and 16 in Fig. 2, that γ increases with decreasing N. This γ-N relation will be exploited in Section 3.

Given the lack of true asymmetric minima in the IBA-1 potential, it is apparent that the asymmetry must arise from dynamical fluctuations due to a softness of the potential in the γ degree of freedom. Examples of such a potential, calculated according to the results of Ref. 9, are shown in Fig. 3, from which it is clear that the deviations of the SU(3) limit from the pure axial rotor, noted above, also arise from this same softness.

For large N values, the curves become steeper and, for $N\to\infty$, are finite only for $\gamma\to 0°$ which is consistent with the above discussion. Figure 3 also shows that, in the IBA-1, there is a necessary relation between γ-softness and mean effective γ so that a large value of one implies a large value of the other. This will have important implications in Section 4.

All of this, of course, raises a difficulty. If asymmetry in the IBA-1 is essentially related to softness, is it correct to extract γ values by comparison with the rigid asymmetric rotor model? To a certain approximation, one must suspect that it is, since it is well known that the Davydov model and the rotor model with dynamic γ-vibrations give similar results when $\gamma_{rigid} = \gamma_{rms}$. Nevertheless, it is an important issue which has been investigated by Castanos, Frank and Van Isacker in Ref. 8 where an alternate method for extracting γ values from the IBA is used which is rigorous and correct for any N. It is based on analytic solutions to the SU(5) limit, expressed in terms of the β and γ shape variables, along with the known expansion of any IBA calculation in the SU(5) basis. Results were obtained[8] for the ground state and are included for comparison in Fig. 2. Clearly, they are not based on a correspondence to a γ-rigid model, yet they do give nearly the same γ-χ correspondence. The small differences between the present calculations and those of Ref. 8 may reflect difficulties with the former but may also reflect a real spin dependence of γ.

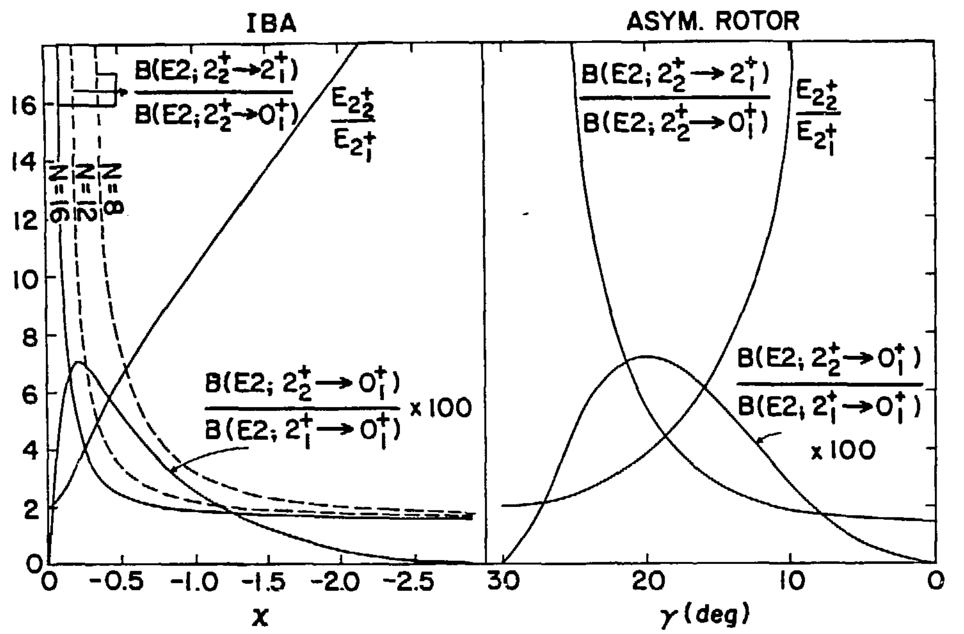

Fig. 1. Energy and B(E2) ratios in the IBA-1 and the asymmetric rotor model.[7] (IBA results for N=16 unless specified.) From Ref. 4.

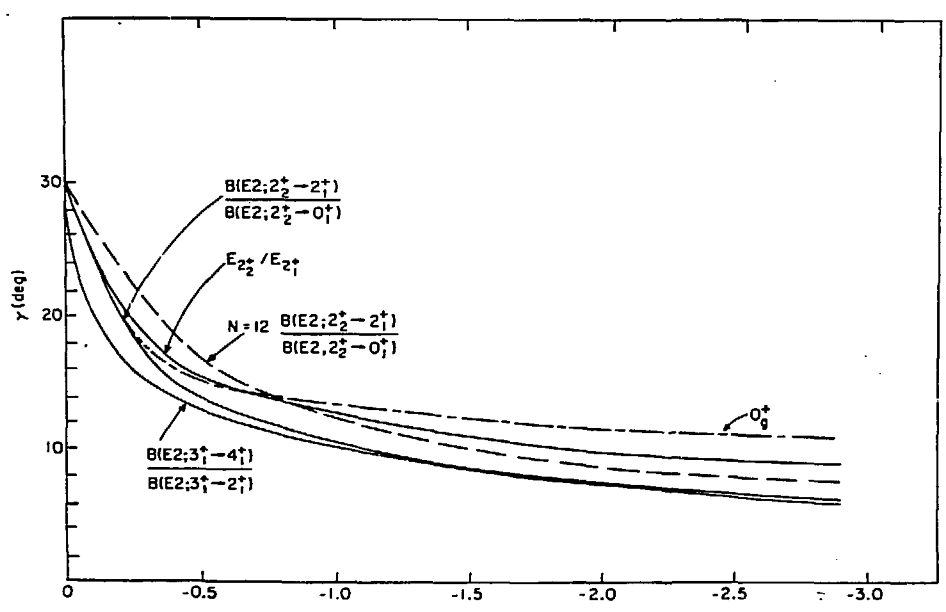

Fig. 2. Asymmetry parameter γ vs. χ for N=16 deduced for several observables as indicated. For one, the results are given for N=12 as well. The curve labelled 0^+_g is taken from Ref. 8 and is based directly on the structure of the ground state wave function.

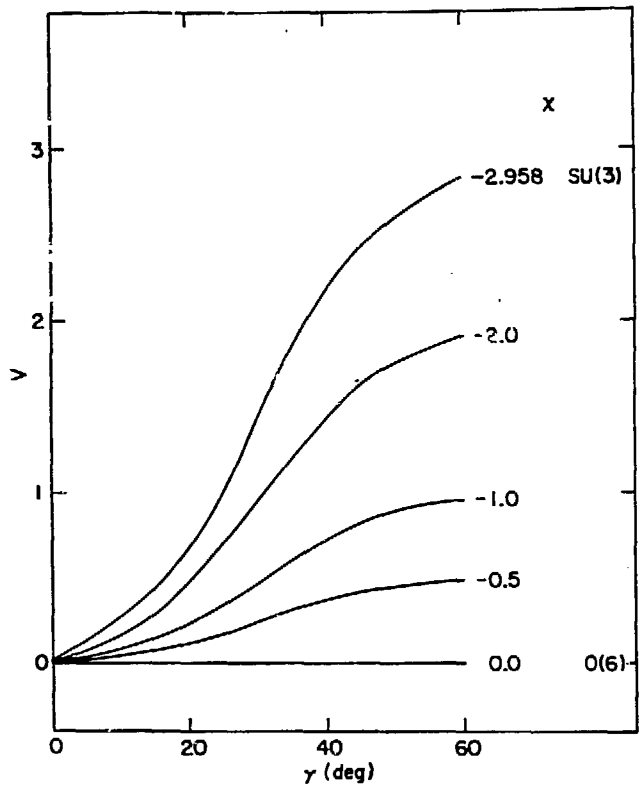

Fig. 3. Schematic illustration of the IBA-1 potential, calculated according to Ref. 9. From Ref. 4.

3. FINITE BOSON NUMBER IN THE IBA

A characteristic feature of the IBA is its explicit incorporation of a finite boson number, N, and of the definition of N as half the sum of the number of valence proton and neutron particles (or holes). Thus, N is fixed for a given nucleus and maximizes at mid-shell. As a consequence, the results of calculations for different N values differ even if the parameters are held constant. This is a crucial feature, and confers, on the ostensibly macroscopic IBA, a microscopic aspect that allows it to generate systematically varying predictions across a shell. The boson number definition is a statement, in effect, that only, but all of, the valence shell is important: that is, intruder orbits from adjacent shells, as well as sub-shell effects within a major shell, are ignored. It is, therefore, an important question whether this basic premise can be supported, that is, whether there is empirical evidence for the variation of boson number with mass and for the correctness of the absolute boson numbers used in the IBA. This section will utilize results related to axial asymmetry to study these questions.

While it was thought at first that boson number effects would be most evident for high spin states, it is now realized that other degrees of freedom enter at high spins, precluding the easy isolation of N-dependent consequences. On the other hand, it has been shown[5] in recent work, which will now be summarized in a slightly altered context to emphasize the relation to asymmetry, that the most evident N-dependent effects appear for low spin states.

The clearest evidence of this should center on systematic varying properties of a series of nuclei so that the extraction of finite N effects is not based on the assumption that the IBA works perfectly for a given nucleus. Also, since most finite N effects are at the few percent level (e.g., intraband B(E2) values), it is crucial to search for particularly sensitive quantities. The easiest empirical results to use are γ-band to ground-band E2 transitions in well deformed nuclei. These are generally well known empirically and, as will be seen, carry a very clear systematics. The key quantities are illustrated in Fig. 4. In a pure harmonic rotor, $\gamma \to g$ branching ratios are given by squares of Clebsch Gordon coefficients (Alaga ratios). In actual nuclei, there are always deviations from these which have been easily explained, in a geometric context, in terms of γ-g bandmixing, whose strength can be expressed by a parameter Z_γ.

A large body of data exists, providing empirical Z_γ values for most rare earth nuclei. These are plotted, against boson number, in Fig. 1 of Ref. 5, and display a remarkable systematics: Z_γ is large near the edges of the shell (small N values) and minimizes at mid-shell (large N). This empirical systematics certainly appears to suggest the relevance of an N dependence but, to prove this, one must show that the IBA reproduces the systematics and does so as a consequence of N effects and not parameter variations.

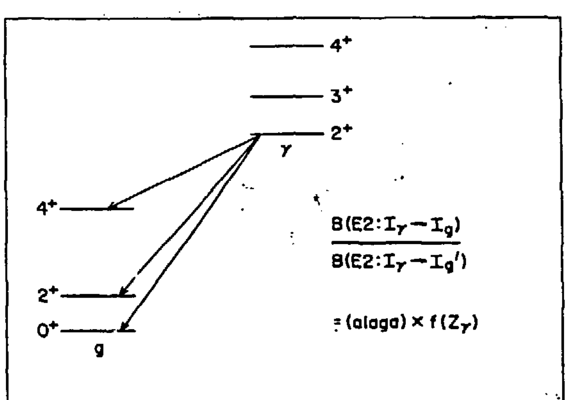

Fig. 4. Illustration of the $\gamma \to g$ band E2 transitions used for discussions of the boson number effects. The expression in the lower right is a schematic representation of the expression for $\gamma \to g$ branching ratios in a geometrical model incorporating γ-g mixing whose spin independent amplitude is proportional to the mixing parameter Z_γ.

It is notable that a natural result of IBA-1 calculations is indeed that $\gamma \to g$ B(E2) values do deviate from the Alaga rules. Thus, one can extract calculated Z_γ values from the IBA and compare them with experimental values. The comparison has been shown in Fig. 4 of Ref. 5 and shows excellent agreement with the data. Here, it is perhaps more interesting to present the same results in slightly different form.

Since Z_γ reflects a γ-g mixing, and since finite values of γ in the asymmetric rotor model lead to K impurities in γ and g band wave functions, one can relate, at least approximately, the two quantities by associating to any γ that Z_γ value that gives the same wave functions or the same value of a given observable. In this way γ values for many deformed nuclei have been obtained. (See, for example, Chapter 7 of Ref. 10.) Similarly, as discussed above, an IBA-1 calculation can be associated with a given γ. Thus, it is possible to compare empirical and IBA predicted γ values. In order to do so, the only prerequisite is the determination of the proper χ values. These have been previously obtained for nuclei from Gd-Pt in Ref. 3 (see Fig. 6 of that paper). It is notable that they are nearly constant (at $\chi \approx -1.1 \pm 0.2$) throughout the region of well deformed nuclei. This is very dramatically clear in the cover illustration for this volume which utilizes a color-coded symmetry triangle to depict the symmetry structure of the rare earth region in the IBA. Aside from the complex structural evolution near Z=64, the O(6) region near ^{196}Pt and the O(6)$\to$rotor transition in Pt-Os, the most evident features of this figure are that the symmetry structure in well deformed nuclei is a) close to but definitely not identical with SU(3) and b) remarkably constant from Gd (for $N \geq 92$) to W. The above mentioned χ values from Ref. 3 have been used to obtain predicted IBA γ values which are compared with experiment in Fig. 5, where the agreement is immediately obvious.

The important point here is that, given the near constancy in χ values, the variations in γ_{IBA} in Fig. 5 are mostly due to the variations in boson number N, thereby demonstrating rather direct experimental evidence confirming the importance of this variation, as embodied in the IBA. (Note that, in geometric models, Z_γ is a phenomenological fitting parameter and has no a priori inherent systematics since such models implicitly correspond to the limit of infinite N.) It is worth noting that the reason the N dependence of γ (or Z_γ) is so strong is somewhat non-trivial but yet fundamental to the structure of the IBA. In deformed nuclei in the IBA, the SU(3) β and g bands mix strongly to produce the calculated resultant ground band. The γ-g transitions then arise partly from an inherent γ-β mixing in SU(3) which varies roughly as $1/N^2$.

In itself, the above discussion does not address the question of the absolute value of N. In principle one could imagine that different parameter choices could produce comparable calculated results for

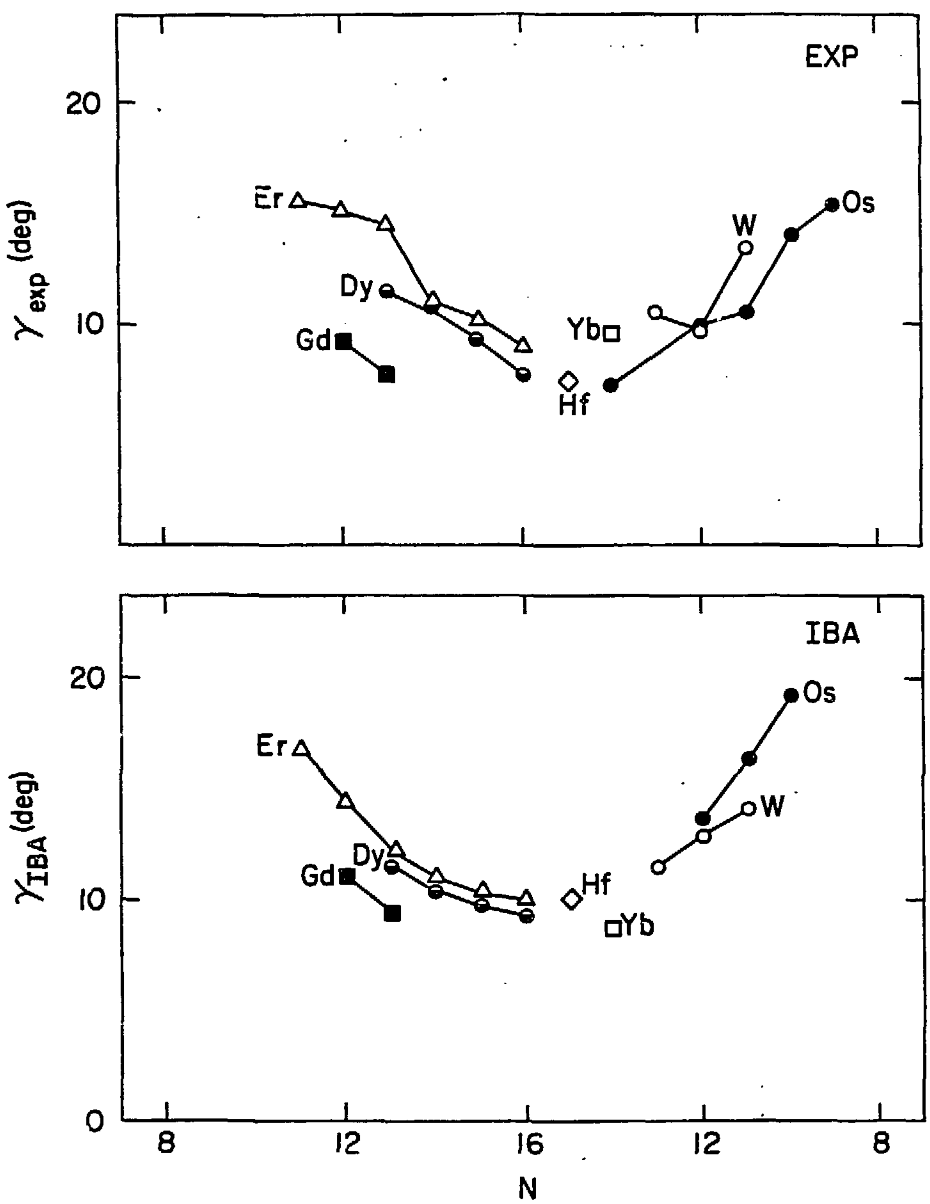

Fig. 5. Comparison of experimental and calculated γ values.

higher or lower N values as long as the variation of N with mass was included. In fact, however, the use of the CQF also provides information on this second question since, in fact, there is no parameter freedom in the context of Eq. (1): the empirical data provide both absolute $\gamma \to g$ B(E2) values, whose scale fixes χ in the CQF, and relative ones (branching ratios), which determine empirical Z_γ or γ values.

Thus, it is possible to perform a set of calculations for a given nucleus as a function of N, as follows. Using the empirical absolute $\gamma \to g$ B(E2) values (in practice, $B(E2{:}2^+_\gamma \to 0^+_g)$), one takes a sequence of N values and extracts, for each, a corresponding χ value. A γ value for every χ and N is then calculated. For six well deformed rare earth nuclei (those with large boson numbers and well defined empirical γ values), these calculations are compared with experiment in Fig. 6. The results all point to the same conclusions. In each case, the best agreement is obtained for absolute boson numbers near those normally defined in the IBA. In all but one case, the calculations agree with experiment for this N value. Most significantly, in each case, the quality of agreement becomes unacceptable (roughly 2 standard deviations) for $N < 3/4\ N_{IBA}$. Once again, it is the consistency of the results, rather than those for any individual nucleus, that lends confidence to these conclusions.

From the standpoint of the IBA, this is a most reassuring result since it tends to confirm one of the basic operational definitions of the model. Note that in providing a rather restrictive lower limit

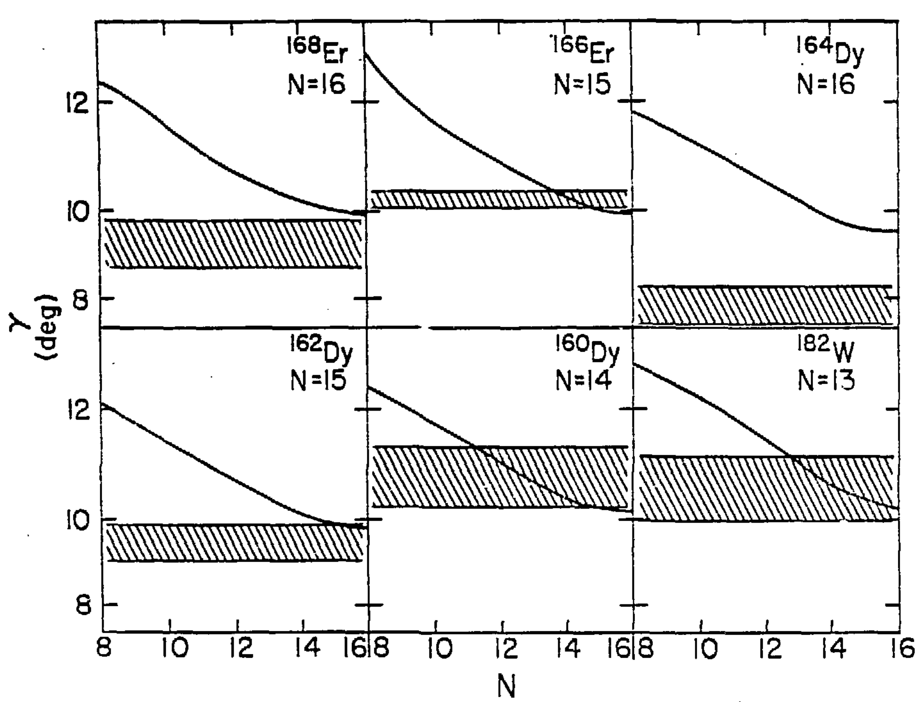

Fig. 6. IBA calculations of γ as a function of boson number N, for several well deformed nuclei (solid lines). The cross hatched bands are the experimental values, including uncertainties. The N values listed in the upper right of each box are the normally defined IBA values. Note the suppressed zero and the non-linearity of the ordinate scale. Based on the second paper in ref. 5.

on N, it does not, however, provide a corresponding upper limit. With the evident flattening of the theoretical curves in Fig. 6, it is clear that these data cannot supply such information. It is possibly obtainable from more transitional nuclei (e.g., W, Os or the light Er isotopes—see Fig. 5) where one suspects that with $N \gg N_{IBA}$ the rapid decrease of γ with N could not be reproduced. However, such a test requires calculations with boson numbers larger than currently feasible and must be deferred. This is unfortunate since it is the more important and controversial aspect of the boson number question (namely, that of restriction to only the valence shell in the IBA). Nevertheless, the present results confirm the need for the inclusion of at least a full major shell and indicate that, for well deformed nuclei, subshell effects are, globally speaking, rather minor, although individual nuclei, such as, ^{172}Yb (see Fig. 5), may reflect their presence.

4. DYNAMIC VS. STATIC ASYMMETRY IN THE IBA: THE MEAN γ/γ SOFTNESS RELATIONSHIP

Axial asymmetry may be obtained in the general context of the IBA in a variety of ways. The simplest is that outlined in Section 2 where it arises naturally, in the usual IBA-1, from the associated softness of the potential in γ. Alternately, the introduction of various complications can lead to asymmetry but, as will be discussed, of a much different type. Recently, three approaches of the latter sort have been used, namely the introduction into the IBA-1 of cubic terms[11] or of g bosons[12] and, into the IBA-2 of quadrupole interactions[13] between like bosons (e.g., $Q_\pi \cdot Q_\pi$). The SU(3)* triaxial symmetry is a limiting case of the latter[13]. In all of these the minimum in the potential of the added interactions is at γ=30°, and one is then dealing with nuclei of stable asymmetric configurations relatively more rigid in γ. The question is if, and how, one can distinguish the origin and effects of asymmetry arising from these different mechanisms.

This questions is nicely illustrated by recent data and calculations for ^{104}Ru, presented in Refs. 14 and 15 by Stachel et al. Figure 7 shows some $\gamma \to g$ band B(E2) values and ground band quadrupole moments in comparison with several calculations including simple IBA-1 ones by Aprahamian[16]. It is clear that symmetric rotor and IBA-2 calculations do not work adequately. However, all those models that incorporate asymmetry (dynamic or static), namely IBA-2*, IBA+g, the asymmetric rotor model and the IBA-1 perform about equally well. Apparently, such transition moments are ideally suited to disclosing evidence for asymmetry but not of its origin. Despite the apparent success of the IBA-1 for the observables in Fig. 7 (and other transition matrix elements), there is one quantity where it disagrees strongly with the data, namely in the energy staggering in the γ band. In a γ-soft potential the energy levels proceed in couplets grouped as (2^+_γ), $(3^+_\gamma 4^+_\gamma)$, $(5^+_\gamma 6^+_\gamma)$ (as in O(6))

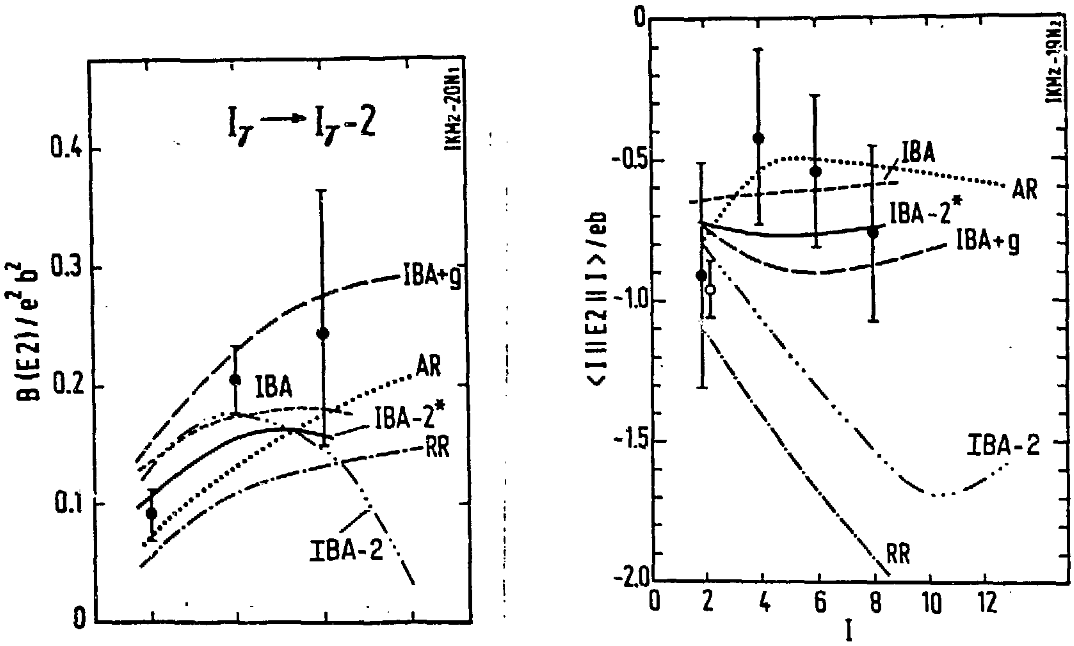

Fig. 7. B(E2) values and ground band quadrupole moments for ^{104}Ru, taken from refs. 14 and 15. The curves labeled IBA are from ref. 16 and were obtained in the CQF with the simple Hamiltonian of eq. (1) modified only to include an εn_d term (EPS (PHINT) = 0.5 MeV) to reflect the structure of ^{104}Ru intermediate between O(6) and SU(5). The χ value was obtained from the γ value deduced in refs. 14 and 15 by utilizing a curve similar to those in Fig. 2, for N=8. The labels AR, RR, IBA-2, IBA-2*, and IBA-g refer the asymmetric rotor, symmetric rotor, standard IBA-2 calculations, IBA-2 calculations incorporating like-boson quadrupole interactions, and IBA-1 calculations incorporating a g boson, respectively.

whereas in a rigid asymmetric rotor, the sequence is closer to $(2^+_\gamma 3^+_\gamma)$, $(4^+_\gamma 5^+_\gamma)$, $(6^+_\gamma 7^+_\gamma)$. The spectrum of ^{104}Ru is intermediate but can be reproduced by extended IBA calculations whereas the IBA-1 necessarily produces an incorrect staggering (see Fig. 3 of Ref. 11).

Since the preceeding pages have dealt only with IBA-1, the issue of IBA-2* will not be considered further here. Also, it has been shown[11] that many of the effects of a g boson can be simulated by cubic terms. Hence, the present discussion will consider only this approach and make use of an extended CQF Hamiltonian of the schematic form

$$H = -\kappa Q\cdot Q + \theta_3 H_{cubic} \qquad (4)$$

where

$$H_{cubic} \approx (d^+d^+d^+)^{(3)}(\tilde{d}\tilde{d}\tilde{d})^{(3)}$$

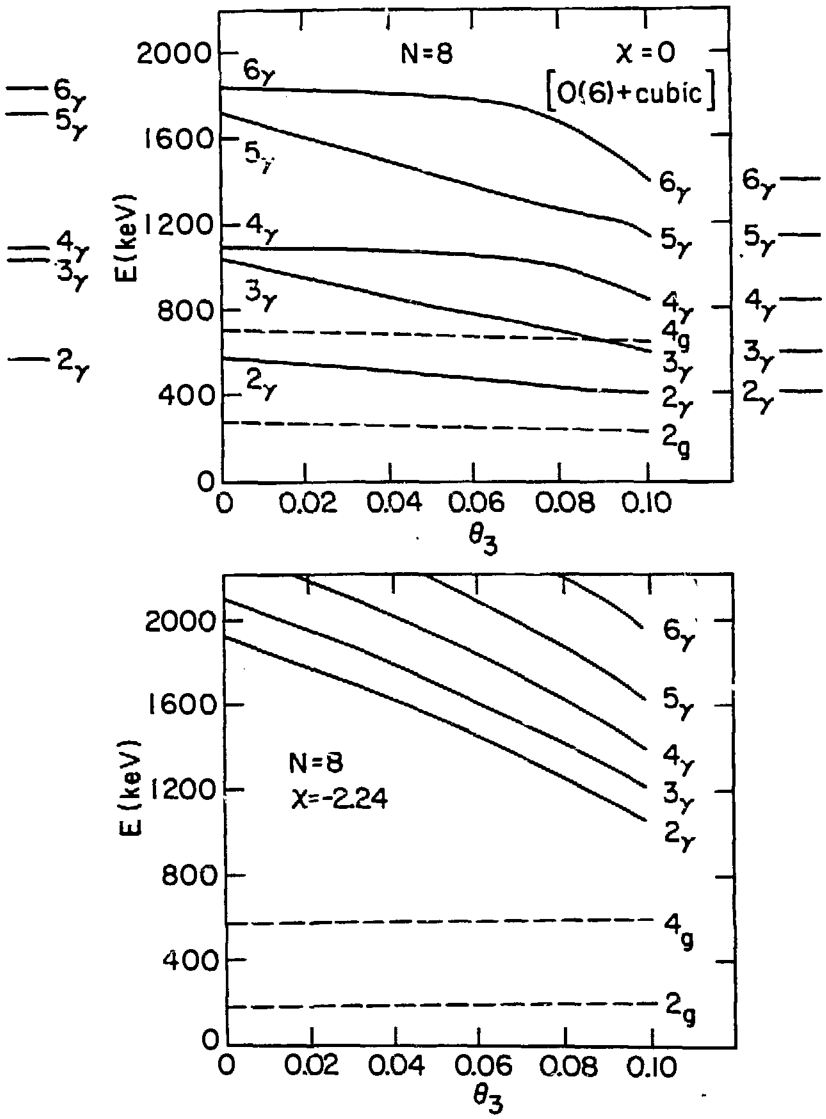

Fig. 8. Ground (dashed) and γ band (solid) energy levels as a function of θ_3 for two values of χ, one corresponding to O(6) and the other to nuclei near SU(3). N=8. In the upper part, the γ band energies for $\theta_3 = 0$ and 0.10 are extracted and displayed on the left and right, respectively.

in order to investigate the systematic evolution of γ band energy staggering as a function of χ and θ_3. It can be anticipated that when θ_3 is small, the potential is γ-soft, and the energy levels of the γ band will behave as in the usual O(6)$\rightarrow$SU(3) transition as χ is varied. For larger θ_3 values the cubic terms will dominate and, even for small χ, one will not obtain an O(6)-like energy staggering. Typical results of these calculations, confirming these expectations, are shown in Fig. 8. Near O(6) (upper part), a small θ_3 leaves the

O(6)-like staggering intact but a more uniform spacing is achieved for larger θ_3. This change in structure results, not so much from a variation in γ but from a decrease in the associated γ-softness as larger θ_3 values lead to a developing potential minimum at $\gamma=30°$. The right side of this figure is not unlike the empirical situation for ^{104}Ru. In the lower part, the IBA potential for $\chi = -2.24$ already has a well defined minimum at $\gamma=0°$ (see Fig. 3) and the effect of the θ_3 term then has a similar effect to the introduction of an increasing γ in the asymmetric rotor model, namely, it rapidly lowers the γ-band energies but without much effect on the staggering. Thus, not surprisingly, the effects of cubic terms on energy staggering are most significant when the IBA potential, excluding such terms, is nearly featureless in γ as is the case near O(6).

These effects also are N dependent. Since the cubic term tends to go as N^3 while the Q·Q interaction goes as N^2, the effect of a given θ_3 is largest for larger N. Indeed, θ_3 values near 0.10 can lead to presumably unphysical states composed solely of d-boson triplets crossing to become the ground state.

It is apparent from these results that the introduction of cubic terms into the IBA-1 hamiltonian leads to a flexibility in the relation between γ-softness and mean γ that is absent from the usual IBA-1. Whether such flexibility is necessary in fitting actual nuclei remains an interesting question. The energy level results for ^{104}Ru suggest that the added complexity (of cubic or g boson terms or of IBA-2*) is needed there. In other regions this may not be true.

5. CONCLUSIONS

The present results may be briefly summarized as follows:

1. The IBA-1 inherently contains an effective finite asymmetry (even in SU(3)).

2. This asymmetry arises from a softness in $V_{IBA}(\gamma)$.

3. It has a strong N dependence, increasing with decreasing N.

4. Point 3 was exploited, using the CQF, to show the importance of boson number variations with mass in the IBA, and to set a lower bound ($N > 3/4\ N_{IBA}$) on acceptable absolute N values.

5. The asymmetry arising automatically from the IBA-1 and from the introduction of higher order terms in the IBA Hamiltonian differs essentially in the associated softness.

6. This difference is chiefly reflected in γ band energy staggering which provides an easy empirical test of the relevance of each type of asymmetry in a given calculation.

7. The combination of the IBA-1 and added cubic terms leads to a flexibility in the mean γ-γ softness relationship. Further work on this relationship is in progress, in particular the construction of contour plots of mean γ and γ-softness against both χ and θ_3 as a function of N.

ACKNOWLEDGEMENTS

I am extremely grateful to A. Aprahamian, D. D. Warner, K. Heyde, P. Van Isacker, and J. Jolie who are my collaborators on this work and who have allowed me to present these results in their names as well. This applies particularly to the still unpublished and preliminary results of Ref. 6 discussed in Section 4. Many enlightening discussions with them, and with Shi Zong-ren, O. Scholten, A. Frank, P. Lipas, and J. Stachel are thankfully acknowledged as is permission from the latter to reproduce figures from Refs. 14 and 15. Lastly, gratitude is due to O. Scholten for his efforts in organizing a very successful conference.

Research has been performed under contract DE-AC02-76CH00016 with the United States Department of Energy.

REFERENCES

1. J. N. Ginocchio, in Interacting Bose-Fermi Systems in Nuclei, ed. F. Iachello (Plenum Press, New York, 1980), p. 179.

2. A. E. L. Dieperink, O. Scholten, and F. Iachello, Phys. Rev. Lett. 44, 1747 (1980).

3. D. D. Warner and R. F. Casten, Phys. Rev. C28, 1798 (1983), and Phys. Rev. Lett. 48, 1385 (1982).

4. R. F. Casten, A. Aprahamian, and D. D. Warner, Phys. Rev. C29 (Rap. Comm.), 356 (1984).

5. R. F. Casten, D. D. Warner, and A. Aprahamian, Phys. Rev. C28, 894 (1983); R. F. Casten and A. Aprahamian, Phys. Rev. C29, 1919 (1984).

6. R. F. Casten, K. Heyde, P. Van Isacker, and J. Jolie, to be published.

7. A. S. Davydov and G. F. Filippov, Nucl. Phys. 8, 237 (1958), and E. P. Grigoriev and M. P. Avotina, Nucl. Phys. 19, 248 (1960).

8. O. Castanos, A. Frank, and P. Van Isacker, Phys. Rev. Lett. 52, 263 (1984).

9. J. N. Ginocchio and M. W. Kirson, Nucl. Phys. A350, 31 (1980).

10. J. M. Eisenberg and W. Greiner, Nuclear Models, Nuclear Theory, Vol. 1 (North Holland, Amsterdam, 1970), Chap. 7.

11. K. Heyde, P. Van Isacker, M. Waroquier, and J. Moreau, Phys. Rev. C29, 1420 (1984).

12. K. Heyde, P. Van Isacker, M. Waroquier, G. Wenes, Y. Gigase, and J. Stachel, Nucl. Phys. A398, 235 (1983).

13. A. E. L. Dieperink and R. Bijker, Phys. Lett. 116B, 77 (1982).

14. J. Stachel, P. Hill, N. Kafrell, H. Emling, H. Grein, E. Grosse, Ch. Michel, H.-J. Wollersheim, D. Schwalm, S. Brussermann, and F. R. May, Nucl. Phys. A419, 589 (1984).

15. J. Stachel, Proc. of the Workshop of Electromagnetic Properties of High Spin Levels, Ein Bokek, Israel, Jan. 9-13, 1984, to be published.

16. A. Aprahamian, private communication.